

## Secondary-ion emission from phenylalanine induced by atomic and molecular MeV ion beams

C. V. Barros Leite, E. F. da Silveira, J. M. F. Jeronymo, R. R. Pinho, and G. B. Baptista  
*Departamento de Física, Pontifícia Universidade Católica, Caixa Postal 38071, Rio de Janeiro 22453, Brazil*

E. A. Schweikert and M. A. Park  
*Center for Chemical Characterization and Analysis, Texas A&M University, College Station, Texas 77843-3144*  
(Received 12 September 1991)

Relative yields of positive and negative secondary ions are measured for atomic and molecular MeV ion beam impinging on a phenylalanine target. The secondary ions were identified by a time-of-flight mass spectrometer.  $C^+$ ,  $O^+$ ,  $CO^+$ , and  $CO_2^+$  were the beams used. The yields obtained for  $[M-H]^-$ ,  $[M+H]^+$ , and  $[M-COOH]^+$  secondary ions show that they are roughly proportional to the third power of the beam stopping power. Other experimental results and predictions of the molecular-expansion model for neutral ejected species are included in the discussion.

### INTRODUCTION

A great effort has been made by several scientists in the attempt to understand the mechanism of sputtering of molecular ions induced by the collision of accelerated ions.<sup>1-18</sup> It is generally accepted that for low-velocity incident ions, lower than the Bohr velocity, the emission of secondary ions depends mainly on the nuclear stopping power.<sup>1,11,16</sup> For ion velocities greater than the Bohr velocity, experimental results indicate that electronic stopping power is responsible for the emission of secondary ions.<sup>2,3,9,14,17</sup> In the abundant literature for slow atomic beams, the linear-cascade theory<sup>1</sup> relates satisfactorily the sputtering yield to the projectile energy loss. On the other hand, for fast and/or molecular beams, literature is scarce and mechanisms for secondary-ion emission are not very well established. In particular, no simple or unique relation between the electronic stopping power and secondary-ion yield gives good agreement with the data in different energy ranges and different combinations of projectile and surface.

In this work experimental results are reported for the yield of the ejection of molecular ions from a phenylalanine target induced by incident ions in the MeV energy range. Some of the incident ions had velocities around the Bohr-velocity values, where data are almost nonexistent. The behavior of the yield as a function of the incident-ion velocity will be discussed and compared with the experimental results of Salehpour, Fishel, and Hunt<sup>14</sup> and with the predictions of a model based on a molecular-dynamics description proposed by Fenyő *et al.*<sup>18</sup> Salehpour, Fishel, and Hunt used  $C^+$ ,  $O^+$ ,  $CO^+$ , and  $CO_2^+$  MeV beams on valine (an amino acid with molecular weight close to phenylalanine) and have analyzed negative secondary molecular ions. Their conclusions are based on the assumption that the secondary-ion yield depends on the square of the electronic stopping power. On the other hand, computer simulations for the electronic sputtering of large neutral molecules from a thin sample carried out by Fenyő *et al.* produced a

third-power dependence of the yield on the stopping power. A similar dependence was obtained by Johnson *et al.*<sup>15</sup> using the pressure-pulse model.

In a recent paper, Brandl *et al.*<sup>19</sup> measured the dependence of secondary-ion yields on the stopping power for several atomic beams with velocity one order of magnitude higher than the Bohr velocity. They found that the yield is proportional to  $(dE/dx - a)^n$ , where  $n$  ranges from 0.5 to 3, depending on the secondary ion and the sample nature. The constant  $a$  is a threshold energy loss.

For lower ion velocities (keV range), some data concerning the phenylalanine target have been reported for atomic ( $Cs^+$ ) and polyatomic ( $Cs_2I^+$ ,  $Cs_3I_2^+$ ) projectiles.<sup>16</sup> It was shown that molecular-ion yields are one order of magnitude higher for polyatomic projectiles with a velocity equal to that of a monoatomic one. This enhancement also occurs with the  $CO^+$  and  $CO_2^+$  projectiles used in the experiment presented here.

### EXPERIMENTAL DETAILS

A time-of-flight (TOF) mass-analysis system was employed to separate and identify the molecular ions sputtered from the sample irradiated with fast ion beams. The primary beams were obtained from a 4-MV Van de Graaff accelerator installed at PUC-Rio. An analyzing magnet selects the ion mass, energy, and charge, and the beam was directed by a switching magnet into the scattering chamber. This switching magnet enables a second analysis of the beam by selecting different charge states resulting from collisions with residual gas along the beam line. The target was placed at a 45° angle of incidence. The overall experimental arrangement is shown schematically in Fig. 1.

Desorbed positive and negative molecular secondary ions were measured for several projectiles with different energies. The desorbed ions were accelerated toward a 20-cm TOF tube by an electric field applied between the target (biased at 2.3 kV) and a grounded grid 5 mm away. The transmission coefficient of the mass spectrometer was

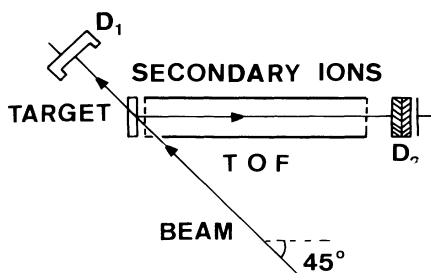


FIG. 1. Setup of the mass spectrometer. The target substrate is a thin film for the positive secondary ions and a metallic grid for negative secondary ions. This last configuration allows the monitoring of molecular beams. The distance from target to grid is 5 mm, and the MCP ( $D_2$ ) detector has its first surface grounded.  $D_1$  is a surface-barrier detector.

not determined, but it is the same for a given secondary ion and for all beams. For the positive secondary ions, the start signal was generated by the incident ion in a silicon detector placed in the beam direction 10 cm after the target. For the negative secondary ions, the electrons emitted from the impact site produced the start signal in the same microchannel detector used for the stop signals. Two different arrangements were used for the coincidence measurements: one using a fast time-to-amplitude converter (TAC) and the other using a time-to-digital converter (TDC). In the first case, only two correlated events can be measured since for each start signal just one stop signal is available for coincidence. In the second case, for each start signal several correlated events can be measured. The results obtained with both arrangements indicate that the emission of just one secondary-ion species for each impact is the dominant effect. The first setup was used for most of the measurements reported here.

Samples of phenylalanine evaporated onto thin films of carbon or Formvar ( $\leq 1000$  Å) coated with aluminum

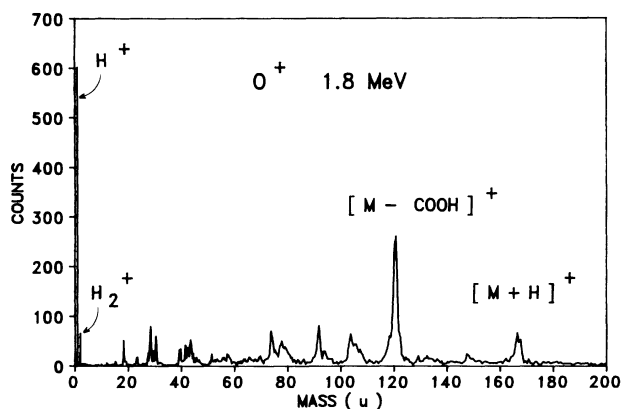


FIG. 2. Typical mass spectrum for positive secondary ions. The beam is  $O^+$  ions of 1.8 MeV energy. The mass calibration was obtained by using the hydrogen-ion peaks. The  $120u$ -mass peak is attributed to the phenylalanine fragment  $[M-COOH]^+$ , and the  $166u$ -mass peak is the protonated molecular ion.

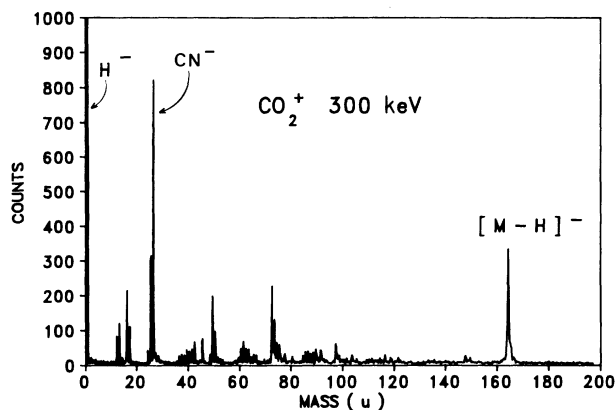


FIG. 3. Typical mass spectrum for negative secondary ions. It corresponds to the 300-keV  $CO_2^+$  molecular-ion beam. The dominant peaks are  $H^-$ ,  $25^-$ , and  $26^-$  hydrocarbon ions and the deprotonated  $166^-$  phenylalanine molecular-ion peak.

and onto a metallic grid were used as targets. The thin films allowed the primary beam to traverse the sample and so to produce the start signal in the silicon detector. The targets prepared on a grid were used for bombardment with the molecular-ion beams and for the measurement of the negative ions ejected. In this situation the secondary ions detected in the MCP detector were uncorrelated to the ions traversing the target. The silicon detector placed after the target was used in this case only to monitor the incident beam. A cold trap was placed at 80 cm from the target in order to minimize the dissociation of the incident molecular ions in the beam line. Typical time-of-flight spectra (converted into mass spectra) are shown in Figs. 2 and 3. Pressure in the chamber was lower than  $10^{-6}$  Torr.

## RESULTS AND DISCUSSION

Samples of phenylalanine, molecular mass  $M=165$ , were bombarded with beams of  $C^+$  and  $O^+$  in the energy range of 0.30 up to 3.0 MeV and with beams of  $CO^+$  and  $CO_2^+$  in the energy range of 0.30 up to 0.90 MeV. The measured relative yields as a function of the velocity of the incident ion for positive-sputtered molecular ions of  $[M+H]^+$  and of  $[M-COOH]^+$  are shown in Fig. 4. Those for negative-sputtered molecular ions  $[M-H]^-$  are shown in Fig. 5. The dashed lines represent the normalized curves for the third power of the stopping power of the ions in the phenylalanine obtained from the Ziegler tables,<sup>23</sup> making use of Bragg's law. The stopping power for molecular ions was obtained by adding the stopping powers for the atomic components of the molecule corresponding to the projectile velocity. Most of the molecular-beam data correspond to a velocity range below the Bohr velocity.

The data presented in Fig. 4 show that the desorption yield of  $M=166^+$  induced by the  $O^+$  beam is roughly 2 times larger than the corresponding yield induced by the  $C^+$  beam. The same ratio is found in data of Fig. 5 for  $M=164^-$  desorbed by  $O^+$  and  $C^+$  beams. In fact, this is also the ratio ( $\sim 2$ ) presented in Ref. 14 for the depro-

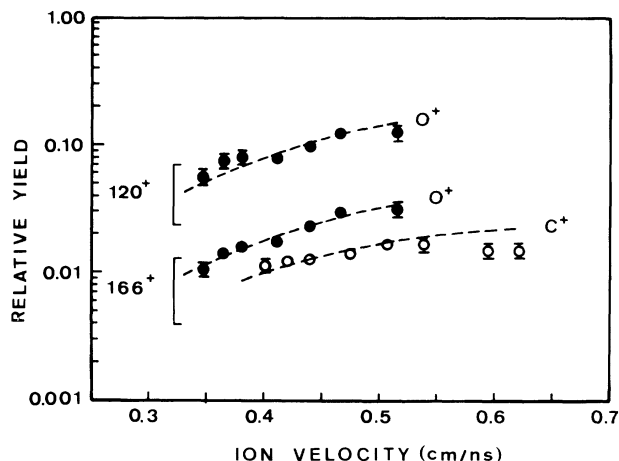


FIG. 4. Relative yields for phenylalanine ( $M=165$ ) positive secondary ions as function of the ion-beam velocity. The 120-mass ion is attributed to the fragment  $[M\text{-COOH}]^+$ , and the 166-mass ion is the protonated ion  $[M+H]^+$ . The dashed lines are the normalized  $(dE/dx)^3$  calculations for oxygen and carbon beams on phenylalanine.

tonated  $M=116^-$  valine ion desorbed by the mentioned beams in the same energy range. It turns out that the calculated electronic stopping-power ratio  $S_O/S_C$  for  $O^+$  and  $C^+$  beams at  $v \approx 0.4$  cm/ns is approximately 1.3. This means that  $(S_O/S_C)^2 \approx 1.7$  and that  $(S_O/S_C)^3 \approx 2.2$ , suggesting that the secondary-ion yield would scale with a stopping power having a power between 2 and 3. When molecular ions are used as projectiles, the situation is similar. In Table I is presented the first, second, and third powers of the ratio  $S/S_C$  of the stopping power  $S$  for several beams to the stopping power for carbon beam,  $S_C$ , calculated also at  $v \approx 0.4$  cm/ns. These values are compared with the results obtained in the present work (for the phenylalanine deprotonated peak  $M=164^-$ ) as well as some results of Salehpour, Fishel, and Hunt<sup>14</sup> (for the valine deprotonated peak  $M=116^-$ ). The experimental results were normalized to the desorption yield corresponding to the  $C^+$  beam,  $Y_C$ .

Assuming  $Y=KS^n$ , the results of Table I indicate that  $n$  would lie between 2 and 3, being even slightly larger than 3 in some cases. Salehpour, Fishel, and Hunt<sup>14</sup> had

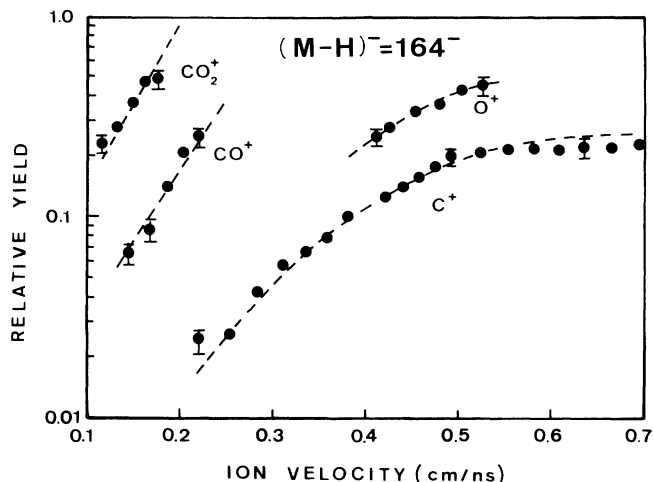


FIG. 5. Relative yields for deprotonated phenylalanine negative secondary ions as a function of atomic- and molecular-ion-beam velocity. The dashed lines are  $(dE/dx)^3$  for the quoted beams.

proposed  $n=2$  based on their data obtained with  $C^+$ ,  $O^+$  and  $Ar^+$  beams, as well as from measurements performed by other groups.<sup>2,5,9,12</sup> They have attributed the larger values of the experimental results, when compared with  $KS^2$ , to enhancements of the electronic stopping power due to collective effects produced by molecular projectiles. This enhancement has also been discussed by others.<sup>20-22</sup>

The results presented by Brandl *et al.*<sup>19</sup> are not directly comparable to ours in the sense that the beam velocities of their measurements are much higher than those presented here. In addition, they have used a carbon foil before the target in order to establish the charge-state equilibrium of the beam. In our measurements all the projectiles were in the  $1+$  charge state, which is below the equilibrium charge state. Nevertheless, we may note that they observed, for a valine target  $n \sim 1.5$  for large positive secondary ions and  $n \sim 2.2$  for negative ones.

The observed third-power dependence of the stopping power matches the prediction of the molecular-expansion model used by Fenyő *et al.*<sup>18</sup> They describe quantitatively the fast ion-induced sputtering of large neutral molecules from samples much thinner than the range of

TABLE I. Comparison of the experimental data from Ref. 14 and from the present work, normalized to the desorption yield  $Y_C$  corresponding to the  $C^+$  beam, with the first-, second-, and third-power ratios of the stopping power  $S$  to the carbon stopping power  $S_C$ . Results from Ref. 14 refer to the valine deprotonated peak  $M=116^-$ , while the present work refers to the phenylalanine deprotonated peak  $M=164^-$ .

Beam	$S/S_C$	$(S/S_C)^2$	$(S/S_C)^3$	$Y/Y_C$	
				Ref. 14	This work
$O^+$	1.3	1.7	2.2	2	2
$O_2^+$	2.6	6.8	18	11	
$C_2^+$	2.0	4.0	8.0	8	
$CO^+$	2.3	5.3	12	9	14
$CO_2^+$	3.6	13	47	22	$\sim 70$

the incident ions on the target materials. These yields were evaluated for incidence angles of  $0^\circ$  and  $45^\circ$ . The data presented in this paper have a similar behavior as a function of the incident-ion stopping power, both for positive and negative molecular ions.

### CONCLUSIONS

Our data indicate that the secondary-molecular-ion yield scales with the electronic stopping power as  $Y \approx KS^n$ , where  $n$  is roughly 3. Salehpour, Fishel, and Hunt,<sup>14</sup> using the same molecular beams and in the same energy ranges, but with another amino-acid target, found the value for  $n$  to be 2. They concluded that, in their case, ion-yield enhancement was due to collective effects. A molecular-dynamics model,<sup>18</sup> in which the sputtering of molecular ions is a result of the molecular expansion

around the beam track, suggests—under certain conditions—a value of 3 for  $n$ . This value corresponds to the behavior exhibited by the present results. Therefore it is clear that more systematic data are needed for a better understanding of the large molecule-emission processes.

Finally, we note that desorption of hydrogen ions follows a different behavior, indicating these ions may be generated by another desorption mechanism.

### ACKNOWLEDGMENTS

This work has been partially supported by SCT, FAPERJ, CNPq, and NSF. The authors acknowledge A. C. M. Gonçalves for stimulating discussions and help in the data acquisition.

<sup>1</sup>P. Sigmund, *Phys. Rev.* **184**, 383 (1969).

<sup>2</sup>P. Dück, H. Fröhlich, W. Treu, and H. Voit, *Nucl. Instrum. Methods* **191**, 245 (1981).

<sup>3</sup>P. Hakansson and B. Sundqvist, *Radiat. Eff.* **61**, 179 (1982).

<sup>4</sup>D. J. Lepoire, B. H. Cooper, C. L. Melcher, and T. A. Tombrillo, *Radiat. Eff.* **71**, 245 (1983).

<sup>5</sup>S. Della-Negra, D. Jacquet, I. Lorthiois, Y. Le Beyec, O. Becker, and K. Wien, *Int. J. Mass. Spectrosc. Ion Phys.* **53**, 215 (1983).

<sup>6</sup>B. Ness, E. Nieschler, N. Bishof, H. Fröhlich, K. Riemer, W. Tiereth, and H. Voit, *Surf. Sci.* **145** 197 (1984).

<sup>7</sup>P. Hakansson, I. Kamensky, M. Salehpour, B. Sundqvist, and S. Widdiyasekera, *Radiat. Eff.* **80**, 141 (1984).

<sup>8</sup>A. Hedin, P. Hakansson, B. Sundqvist, and R. E. Johnson, *Phys. Rev. B* **31**, 1780 (1985).

<sup>9</sup>O. Becker, S. Della-Negra, Y. Le Beyec, and K. Wien, *Nucl. Instrum. Methods B* **16**, 321 (1986).

<sup>10</sup>R. E. Johnson, *Int. J. Mass. Spectrosc. Ion Phys.* **78**, 357 (1987).

<sup>11</sup>I. S. Bitensky and E. S. Parilis, *Nucl. Instrum. Methods B* **21**, 26 (1987).

<sup>12</sup>S. Della-Negra, O. Becker, R. Cotter, Y. Le Beyec, B. Monart, K. Standing, and K. Wien, *J. Phys. (Paris)* **48**, 151 (1987).

<sup>13</sup>A. Hedin, P. Hakansson, M. Salehpour, and B. Sundqvist, *Phys. Rev. B* **35**, 7377 (1987).

<sup>14</sup>M. Salehpour, D. Fishel, and J. Hunt, *Phys. Rev. B* **38**, 12 320 (1988).

<sup>15</sup>R. E. Johnson, B. Sundqvist, A. Hedin, and D. Fenyö. *Phys. Rev. B* **40**, 49 (1989).

<sup>16</sup>M. G. Blain, S. Della-Negra, H. Joret, Y. Le Beyec, and E. A. Scheweikert, *Phys. Rev. Lett.* **63**, 1625 (1989).

<sup>17</sup>J. P. Thomas, A. Oladipo, and M. Fallavier, *J. Phys. (Paris) Colloq.* **50**, C2-195 (1989).

<sup>18</sup>D. Fenyö, B. Sundqvist, B. R. Karlsson, and R. E. Johnson, *Phys. Rev. B* **42**, 1895 (1990).

<sup>19</sup>D. Brandl, Ch. Shoppmann, R. Schmidt, B. Ness, A. Ostrowski, and H. Voit, *Phys. Rev. B* **43**, 5253 (1991).

<sup>20</sup>W. Brandt, A. Ratkowski, and R. H. Ritchie, *Phys. Rev. Lett.* **33**, 1325 (1974).

<sup>21</sup>J. W. Tape, W. M. Gibson, J. Remillieux, R. Laubert, and H. E. Wegner, *Nucl. Instrum. Methods* **132**, 75 (1976).

<sup>22</sup>N. R. Arista, *Phys. Rev. B* **18**, 1 (1978).

<sup>23</sup>J. F. Ziegler, *Handbook of Stopping Cross Sections for Energetic Ions in All Elements* (Pergamon, New York, 1980); J. P. Biersack and J. F. Ziegler, TRIM code (unpublished).